Acta Crystallographica Section F
Structural Biology and Crystallization Communications
ISSN 1744-3091

Heterodimeric nitrate reductase (NapAB) from *Cupriavidus necator* H16: purification, crystallization and preliminary X-ray analysis

Catarina Coelho,[a] Pablo J. González,[a] José Trincão,[a] Ana L. Carvalho,[a] Shabir Najmudin,[a] Thomas Hettman,[b] Stephan Dieckman,[b] José J. G. Moura,[a] Isabel Moura[a] and Maria J. Romão[a]*

[a]REQUIMTE/CQFB, Departamento de Química, Faculdade de Ciências e Tecnologia, Universidade Nova de Lisboa, 2829-516 Caparica, Portugal, and [b]Institute for Molecular Biotechnology, Beutenbergstrasse 11, 07745 Jena, Germany

Correspondence e-mail: mromao@dq.fct.unl.pt

Received 12 February 2007
Accepted 4 May 2007

The periplasmic nitrate reductase from *Cupriavidus necator* (also known as *Ralstonia eutropha*) is a heterodimer that is able to reduce nitrate to nitrite. It comprises a 91 kDa catalytic subunit (NapA) and a 17 kDa subunit (NapB) that is involved in electron transfer. The larger subunit contains a molybdenum active site with a bis-molybdopterin guanine dinucleotide cofactor as well as one [4Fe–4S] cluster, while the small subunit is a di-haem *c*-type cytochrome. Crystals of the oxidized form of this enzyme were obtained using polyethylene glycol 3350 as precipitant. A single crystal grown at the High Throughput Crystallization Laboratory of the EMBL in Grenoble diffracted to beyond 1.5 Å at the ESRF (ID14-1), which is the highest resolution reported to date for a nitrate reductase. The unit-cell parameters are a = 142.2, b = 82.4, c = 96.8 Å, $\beta = 100.7^{\circ}$, space group $C2$, and one heterodimer is present per asymmetric unit.

1. Introduction

Nitrate reductases are mononuclear molybdenum-containing enzymes that reduce nitrate to nitrite in a two-electron reduction process. In addition to the Mo active site, they have additional redox cofactors such as iron–sulfur and haem centres that mediate electron-transfer reactions between the electron donor and nitrate. The Mo atom is part of a cofactor referred to as molybdopterin. Enzymes dependent on this cofactor have been grouped into three families represented by (i) xanthine oxidase, (ii) sulfite oxidase and (iii) DMSO reductase (Hille, 1996).

Nitrate reductases are quite diverse in terms of subunit composition, active-site structure, cellular localization and physiological function. In prokaryotes, they have been classified into three groups: cytoplasmic assimilatory nitrate reductases (Nas), membrane-bound respiratory nitrate reductases (Nar) and periplasmic nitrate reductases (Nap) (Berks *et al.*, 1995; Stolz & Basu, 2002; Gonzalez *et al.*, 2006). While the prokaryotic enzymes belong to the DMSO reductase family of molybdenum enzymes, those found in eukaryotes belong to the sulfite oxidase family.

With the exception of the monomeric NapA from *Desulfovibrio desulfuricans* ATCC 27774 (Dias *et al.*, 1999), the periplasmic nitrate reductases characterized to date are usually found in association with a small subunit that is involved in electron transfer. The catalytic subunit NapA (~70–90 kDa) contains a bis-MGD (molybdopterin guanine dinucleotide) cofactor bound to the Mo atom and one [4Fe–4S] centre. In the oxidized form, the active site is formed by a distorted hexacoordinated Mo^{VI} ion, in which the metal atom is coordinated by four S atoms from two dithiolene ligands (MGD), one hydroxo/water/sulfido ligand and a cysteinyl ligand from the protein.

Three crystal structures of periplasmic nitrate reductases are currently known. The monomeric NapA from *D. desulfuricans* (*Dd* NapA) was the first to be published (Dias *et al.*, 1999) and was solved to a resolution of 1.9 Å. In 2003, Arnoux and coworkers reported a low-resolution (3.2 Å) structure of the NapAB complex from *Rhodobacter sphaeroides* (*Rs* Nap; Arnoux *et al.*, 2003) and very recently the 2.5 Å crystal structure of *Escherichia coli* NapA was published (*Ec* NapA; Jepson *et al.*, 2007). In the latter case the two subunits NapA and NapB were purified independently, but only NapA was crystallized. *Cupriavidus necator* NapA (*Cn* NapA) shares

36% sequence identity to *Dd* NapA, 69% to *Ec* NapA and 72% to *Rs* NapA. The sequence of *Cn* NapB is 52% identical to that of *Rs* NapB. The three-dimensional structures of the catalytic subunits of *Dd* NapA, *Rs* NapA and *Ec* NapA are very similar in terms of metal-cofactor content, global fold and domain organization. The residues at the active-site cavity and at the funnel which leads to the Mo site are conserved, as well as those involved in the Mo–bis-MGD and [4Fe–4S] binding.

The genes for the periplasmic nitrate reductase from *C. necator* are not part of the bacterial chromosome, but are located on the megaplasmid pHG1 present in the wild-type strain H16. For expression of *Cn* NapAB, a megaplasmid-free strain (HF210) was used, into which a broad host-range vector (pCM62) containing the complete *nap* cluster (pTH200) was inserted (Hettmann *et al.*, 2003). *Cn* NapAB consists of a 91 kDa catalytic NapA subunit and a 17 kDa di-haem *c*-type cytochrome NapB subunit (Siddiqui *et al.*, 1993). Here, we report the expression, purification and crystallization of this heterodimeric NapAB. The diffraction data to 1.5 Å resolution will provide a better description of the whole complex and in particular a clearer picture of the structural details at and near the catalytic site. In addition, the available expression system as well as the improved purification protocol will enable us to complement these studies with other forms of the enzyme (reduced, substrate analogue-bound and inhibitor-bound forms), which will be an important contribution towards the clarification of the reaction mechanism of this family of nitrate reductases and will allow functional comparison with other nitrate reductases.

2. Materials and methods

2.1. Purification

C. necator HF210-pTH200 was grown in mineral medium as described previously (Siddiqui *et al.*, 1993). *Cn* NapAB (gene IDs NapA 2656653 and NapB 2656654, respectively) was purified from the periplasmic extract. To isolate the periplasm, the culture was centrifuged at 5000*g* for 20 min. The pellet was washed in 50 m*M* Tris–HCl pH 7.6 and resuspended in 10 m*M* Tris–HCl pH 7.6, 0.5 *M* sucrose (5 ml per gram of pellet). EDTA was added to a final concentration of 1 m*M* and the cells were incubated at 303 K for 10 min with slow shaking. Lysozyme was added (20 mg per gram of pellet) and the cells were stirred vigorously for 30 min at room temperature. The resulting suspension was centrifuged for 20 min at 5000*g*. The supernatant contained the periplasmic extract, which was dialyzed overnight against 10 m*M* MES pH 5.5. The sample was then loaded onto a Source 15S column (GE-Amersham). *Cn* NapAB eluted between 200 and 250 m*M* NaCl. After concentration, the protein was injected onto a Superdex 200 column pre-equilibrated with 100 m*M* Tris–HCl pH 7.6. The fraction containing the protein was dialyzed against 10 m*M* MES pH 5.5 and loaded onto a Source

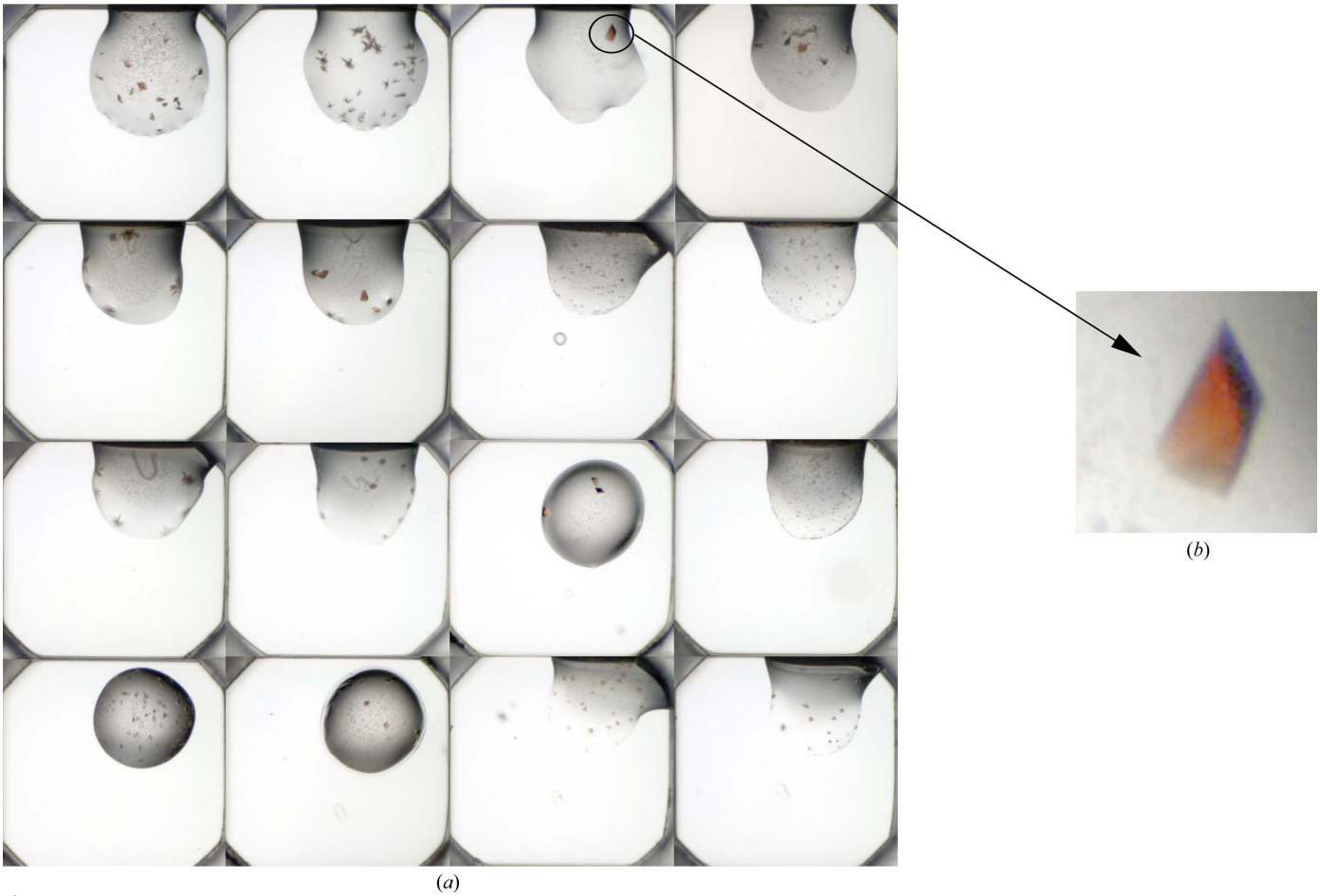

(*a*) (*b*)

Figure 1
Crystals obtained using the crystallization robot. (*a*) From left to right and top to bottom, Index Screen condition Nos. 41, 65, 89, 42, 82, 90, 43, 91, 84, 93, 46, 78, 86, 47, 71 and 87. (*b*) Enlargement of crystallization condition No. 89, crystal dimensions 0.13 × 0.09 × 0.04 mm.

Table 1
Data-collection statistics.

Values in parentheses are for the highest resolution shell.

X-ray source	ID14-1 (ESRF, Grenoble)
Crystal data	
Crystal system	Monoclinic
Unit-cell parameters (Å, °)	a = 142.2, b = 82.4, c = 96.8, β = 100.7
Maximum resolution (Å)	1.5
Mosaicity (°)	0.57
Molecules (AB dimer) per ASU	1
Matthews coefficient (Å^3 Da^{-1})	2.53
Data collection and processing	
Space group	$C2$
Wavelength (Å)	0.934
No. of observed reflections	645330 (92176)
No. of unique reflections	170014 (254265)
Resolution limits (Å)	43.23–1.50 (1.58–1.50)
Redundancy	3.8
R_{sym}† (%)	0.085 (0.537)
Completeness (%)	97.2 (95.2)
$\langle I/\sigma(I)\rangle$	8.5 (2.3)

† $R_{sym} = \sum_{\mathbf{h}}\sum_l |I_{\mathbf{h}l} - \langle I_{\mathbf{h}}\rangle| / \sum_{\mathbf{h}}\sum_l \langle I_{\mathbf{h}}\rangle$, where I_l is the lth observation of reflection **h** and $\langle I_{\mathbf{h}}\rangle$ is the weighted average intensity for all observations l of reflection **h**.

15S column (GE-Amersham). NapAB was eluted between 200 and 250 m*M* NaCl. The buffer was exchanged to 10 m*M* Tris–HCl pH 7.6 during concentration to a final protein concentration of 10 mg ml^{-1}.

2.2. Crystallization

Initial crystallization conditions were screened at the High Throughput Crystallization Laboratory at EMBL, Grenoble. The experiments were set up with a Cartesian PixSys 4200 crystallization robot (Genomic Solutions, UK) using the Index Screen from Hampton Research at 293 K. Crystals were obtained using the sitting-drop vapour-diffusion method in several different conditions (Fig. 1*a*). The best crystals (conditions 89 and 42) were produced in 15 and 25%(*w*/*v*) PEG 3350, 0.1 *M* bis-Tris pH 5.5 or 0.1 *M* succinic acid pH 7.0. The crystals grew within one week to approximate dimensions of 0.13 × 0.09 × 0.04 mm (Fig. 1*b*) by mixing 100 nl protein solution (10 mg ml^{-1}) with an equal volume of precipitant and equilibrating over 90 µl reservoir solution. Attempts are now being carried out to reproduce and scale up these conditions in-house using a larger drop volume.

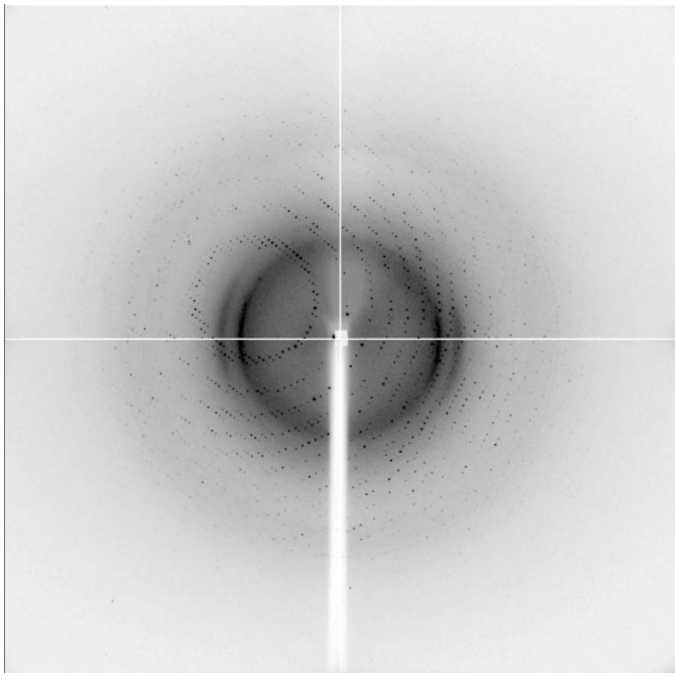

Figure 2
Diffraction pattern of the NapAB crystal (the resolution at the edge is 1.5 Å) obtained at beamline ID14-1 (ESRF).

2.3. Data collection and processing

Crystals were flash-cooled directly in liquid nitrogen prior to transfer to a gaseous nitrogen stream (100 K), using Paratone oil as a cryoprotectant. A high-resolution data set was obtained at beamline ID14-1 at the European Synchrotron Radiation Facility (ESRF, Grenoble, France) using an ADSC Quantum-4R CCD detector. The crystals diffracted to beyond 1.5 Å at a wavelength of 0.934 Å (Fig. 2). They belong to space group $C2$, with unit-cell parameters a = 142.2, b = 82.4, c = 96.8 Å, β = 100.7°. The data were processed using *MOSFLM* v.6.2.5 (Leslie, 1992) and *SCALA* (Kabsch, 1988) from the *CCP*4 program package v.6.0 (Collaborative Computational Project, Number 4, 1994). Matthews coefficient calculations suggest the presence of one heterodimer per asymmetric unit (V_M = 2.53 Å^3 Da^{-1}; Matthews, 1968) and a solvent content of ∼51.5%. Data-collection and processing statistics are presented in Table 1.

3. Results and discussion

Periplasmic nitrate reductase from *C. necator* was purified to near-homogeneity. Because of the low yields of the expression (0.2 mg of protein were obtained from 18 l culture), the crystallization trials were performed at the High-Throughput Crystallization facility in order to maximize the number of trials by minimizing the drop volume and the amount of protein sample. Several crystallization conditions were obtained using Index Screen from Hampton Research (Fig. 1*a*). The two best conditions yielded crystals that were large enough to be handled and were successfully mounted on a loop. Diffraction data from these crystals were collected at ID14-1 (ESRF) to a resolution beyond 1.5 Å, which is the highest resolution to be obtained to date for a nitrate reductase. The crystals belong to space group $C2$, with unit-cell parameters a = 142.2, b = 82.4, c = 96.8 Å, β = 100.7°. The calculated Matthews coefficient is 2.53 Å^3 Da^{-1}, suggesting the presence of one AB dimer in the asymmetric unit (Matthews, 1968). Molecular replacement was performed using *Dd* NapA (Dias *et al.*, 1999; PDB code 2nap; the full model was used, not including the MGD and the [4Fe–4S] cofactors), as a search model and the molecular-replacement program *Phaser* (McCoy *et al.*, 2005; Read, 2001). A clear solution was obtained, allowing the identification of clear density for the Mo–bis-MGD, the [4Fe–4S] centre and the NapB subunit. Calculation of an anomalous map shows clear density for the Mo, the Fe atoms of the [4Fe–4S] centre and the Fe atoms of the two *c*-type haems of NapB, confirming the presence of the dimer in the crystal.

This work was financially supported by the Portuguese Science and Technology Foundation (FCT-MCTES) through project POCI/QUI/57641/2004 financed by the program POCI2010 and co-financed by FEDER and grants SFRP/BD/10825/2002 (PJG) and SFRH/BPD/20357/2004 (SN). The authors would like to thank the ID14-1 staff of the ESRF (Grenoble, France) for assistance during data collection. Special thanks are given to Dr Jose A. Marquez of the High Throughput Crystallization Laboratory (EMBL, Grenoble) for help during crystal retrieval at the ESRF.

References

Arnoux, P., Sabaty, M., Alric, J., Frangioni, B., Guigliarelli, B., Adriano, J. M. & Pignol, D. (2003). *Nature Struct. Biol.* **10**, 928–934.

Berks, B. C., Page, M. D., Richardson, D. J., Reilly, A., Cavill, A., Outen, F. & Ferguson, S. J. (1995). *Mol. Microbiol.* **15**, 319–331.

Collaborative Computational Project, Number 4 (1994). *Acta Cryst.* D**50**, 760–763.

Dias, J. M., Than, M. E., Humm, A., Huber, R., Bourenkov, G. P., Bartunik, H. D., Bursakov, S., Calvete, J., Caldeira, J., Carneiro, C., Moura, J. J., Moura, I. & Romao, M. J. (1999). *Structure*, **7**, 65–79.

Gonzalez, P. J., Rivas, M. G., Brondino, C. D., Bursakov, S. A., Moura, I. & Moura, J. J. (2006). *J. Biol. Inorg. Chem.* **11**, 609–616.

Hettmann, T., Siddiqui, R. A., von Langen, J., Frey, C., Romao, M. J. & Diekmann, S. (2003). *Biochem. Biophys. Res. Commun.* **310**, 40–47.

Hille, R. (1996). *Chem. Rev.* **96**, 2757–2816.

Jepson, B. J., Mohan, S., Clarke, T. A., Gates, A. J., Cole, J. A., Butler, C. S., Butt, J. N., Hemmings, A. M. & Richardson, D. J. (2007). *J. Biol. Chem.* **282**, 6425–6437.

Kabsch, W. (1988). *J. Appl. Cryst.* **21**, 916–924.

Leslie, A. G. W. (1992). *Jnt CCP4/ESF–EACBM Newsl. Protein Crystallogr.* **26**.

McCoy, A. J., Grosse-Kunstleve, R. W., Storoni, L. C. & Read, R. J. (2005). *Acta Cryst.* D**61**, 458–464.

Matthews, B. W. (1968). *J. Mol. Biol.* **33**, 491–497.

Read, R. J. (2001). *Acta Cryst.* D**57**, 1373–1382.

Siddiqui, R. A., Warnecke-Eberz, U., Hengsberger, A., Schneider, B., Kostka, S. & Friedrich, B. (1993). *J. Bacteriol.* **175**, 5867–5876.

Stolz, J. F. & Basu, P. (2002). *Chembiochem*, **3**, 198–206.